Lattice meson electric form factor using Wilson fermions

R. M. Woloshyn
TRIUMF, 4004 Wesbrook Mall, Vancouver, British Columbia, Canada V6T 2A3
(Received 5 December 1985)

The electric form factor of the pseudoscalar meson (generic pion) is calculated in quenched lattice quantum chromodynamics with SU(2) color using the Wilson formulation for fermions. Charge radii are calculated for different values of the hopping parameter. It is observed that heavier quarks have distributions of smaller radius. The results are compared with a previous calculation which used the staggered fermion scheme.

I. INTRODUCTION

The methods of lattice quantum chromodynamics (QCD) are now well established[1] and are being widely applied. However, the best way of dealing with fermion fields on the lattice is still not clear. The problem arises because locality, explicit chiral invariance of the action, and suppression of species doubling cannot be imposed simultaneously[2,3] At present the Wilson scheme,[4] which avoids species doubling, and the staggered formulation,[5–7] which preserves a remnant of chiral symmetry, are commonly used in Euclidean lattice QCD simulations. Of course, in the continuum limit it is expected that the differences between these schemes are irrelevant. It is important, at finite lattice spacing, to demonstrate that the same physical results can be obtained with different lattice fermion formulations, or, at least, that the differences can be understood and ultimately controlled. To some extent this has already been done for mass spectrum calculations.[8] Recently there has been some progress in the study of lattice hadron structure[9,10] and it is natural to ask how these results depend on the way in which fermions were put on the lattice.

Hadron form factors, extracted from the vector current three-point function, are a useful probe of hadron structure. They can be calculated in lattice QCD in a (color) gauge-invariant way and, ultimately, are directly comparable to experimental result. In Ref. 10 it was shown how to calculate the electric form factor for the pseudo-Goldstone boson (a generic pion) on the lattice. A detailed study[11] of the pseudoscalar-meson electric form factor, and the charge radius extracted from it, was carried out as a function of quark mass with the physically reasonable result that heavier quarks have distributions of smaller radius. The calculations of Ref. 11 were done using the staggered scheme for lattice fermions. In the present paper a similar study of the form factor is done using Wilson fermions. The calculation is done in a way (e.g., using the same gauge field configurations) that the results can be compared with the previous staggered fermion calculation.

In Sec. II expressions for the vector current three-point function and the meson electric form factor are derived. With Wilson fermions the derivation is much more straightforward than in the staggered case.[12] Since, in the Wilson scheme, there is a Dirac field associated with every lattice site one can start with hadron interpolating fields that are local. In contrast, the staggered scheme requires construction of Dirac fields on hypercubes in the lattice. Considerable effort is then required to reduce the three-point function to a form involving effectively local operators.[12] This leads in the staggered scheme to lattice matrix elements with contributions from states of different parity. In the Wilson scheme this problem does not occur. The final result of Sec. II is an expression for the electric form factor in terms of three-point and two-point hadron correlation functions.

Section III contains details of the numerical work and the results. The calculations were done for quenched approximation in a model with SU(2) color (at $\beta=2.3$) and use gauge field configurations that were also used in Ref. 11. Five different values of the hopping parameter, from $\kappa=0.134$ to $\kappa=0.158$, were used. The electric form factor was calculated for a flavor-nonsinglet 0^- meson. The charge radius was calculated from the derivative of the form factor at zero-momentum transfer. Form factors and charge radii are presented for a meson constructed from an equal-mass quark-antiquark pair and also for the case of unequal-mass quark and antiquark. The qualitative features of the results, e.g., the decrease in the radius of the quark distribution with increasing mass, are the same as observed with staggered fermions.

A more detailed comparison of the present results with those of Ref. 11 is given in Sec. IV. A superficial examination of charge radius versus mass in lattice units would suggest that Wilson and staggered fermions give different results. If the results are converted to physical units by fixing the length scale using pion and ρ-meson masses, the charge radii become quite compatible. However, the length scales that emerge for the Wilson and staggered schemes come out to be quite different, indicating, perhaps, that one is still quite far from continuum physics.

Finally it should be noted that information about charge distributions can also be extracted from charge-density correlations.[13] This has been done for pseudoscalar mesons using the Wilson scheme. The results presented in this paper are compatible with those of Ref. 13.

II. FORMALISM

In this section the relevant formulas for calculating the two-point and three-point functions are given. The Wilson scheme[4] for lattice fermions is used. Two flavors of quarks (called u and d) are introduced. The Wilson fermion action is (suppressing color and Dirac indices)

$$S_F(u)=\bar{\psi}M\psi$$
$$=\sum_{x,\mu,f=\{u,d\}}\kappa_f[\bar{\psi}^f(x)(r+\gamma_\mu)U_\mu(x)\psi^f(x+a_\mu)+\bar{\psi}^f(x+a_\mu)(r-\gamma_\mu)U_\mu^\dagger(x)\psi_\mu^f(x)]-\sum_{x,f}\bar{\psi}^f(x)\psi^f(x), \quad (1)$$

where a_μ is the unit vector in the μ direction and κ_f is the hopping parameter. The coefficient of the Wilson term r will be put equal to 1 in numerical calculations. The fermion matrix M is diagonal in flavor and satisfies the relation[14]

$$\gamma_5 M^\dagger\gamma_5=M, \quad (2)$$

where γ_5 acts on Dirac indices. For SU(2) the relation[15]

$$\gamma_5\gamma_2\sigma_2 M\sigma_2\gamma_2\gamma_5=M^*, \quad (3)$$

with σ_2 acting on color indices, is also satisfied.

The fermion action is invariant under global transformation

$$\psi^f(x)\rightarrow e^{i\omega^f}\psi^f(x), \quad (4a)$$
$$\bar{\psi}^f(x)\rightarrow\bar{\psi}^f(x)e^{-i\omega^f} \quad (4b)$$

for each flavor. Using the Noether procedure a conserved vector current can be derived. The result is (for each flavor, $f=u$ or d)

$$j_\mu^f(x)=-i\kappa_f[\bar{\psi}^f(x)(r+\gamma_\mu)U_\mu(x)\psi^f(x+a_\mu)$$
$$-\bar{\psi}^f(x+a_\mu)(r-\gamma_\mu)U_\mu^\dagger(x)\psi^f(x)], \quad (5)$$

An advantage of the Wilson scheme over staggered fermions is that local composite hadron operators with definite quantum numbers can be defined. For the flavor-nonsinglet pseudoscalar meson the operator

$$O_0=\bar{\psi}^u(x)\gamma_5\psi^d(x) \quad (6)$$

is used. For the vector meson (generic ρ-meson) we use

$$O_1^i=\bar{\psi}^u(x)\gamma_i\psi^d(x). \quad (7)$$

The correlation function

$$G_J(\mathbf{p},t_x)=\sum_{\mathbf{x}}e^{-i\mathbf{p}\cdot\mathbf{x}}\langle O_J(x)O_J^\dagger(0)\rangle, \quad (8)$$

with

$$\langle\cdots\rangle=Z^{-1}\int dU\,d\bar{\psi}\,d\psi\,e^{-S_G-S_F}(\cdots) \quad (9)$$

and S_G equal to the gauge field action, describes the propagation of meson states with momentum $\mathbf{p}$. At large time separation

$$G_J(\mathbf{p},t_x)\rightarrow\langle\Omega_+|O_J(0)|J,\mathbf{p}\rangle\langle J,\mathbf{p}|O^\dagger(0)|\Omega_-\rangle e^{-E_pt_x} \quad (10a)$$
$$\rightarrow C_+(J,\mathbf{p})C_-(J,\mathbf{p})e^{-E_pt_x}, \quad (10b)$$

where $|J,\mathbf{p}\rangle$ denotes the meson state with spin J and momentum $\mathbf{p}$, and $E_p=(\mathbf{p}^2+M_J^2)^{1/2}$. In the numerical calculation a nonperiodic boundary condition is used in the time direction. Quarks are not allowed to propagate across the time edges of the lattice. This introduces nonvacuum contamination[16] into the correlation functions and is the reason why a distinction is made between left and right vacua ($\Omega_\pm$) in (10).

To get the pseudoscalar-meson electric form factor we calculate the three-point function

$$A(\mathbf{p},\mathbf{q},t_x,t_z)=\sum_{\mathbf{x}}e^{-i\mathbf{p}\cdot\mathbf{x}}\times\left\langle O_0(x)\sum_{\mathbf{z}}e^{i\mathbf{q}\cdot\mathbf{z}}\rho(z)O_0^\dagger(0)\right\rangle, \quad (11)$$

where the charge-density operator is

$$\rho(z)=i[q^dj_4^d(z)+q^uj_4^u(z)] \quad (12)$$

with q^d,q^u equal to the quark charges ($q^u-q^d=1$). At large time separation $0\ll t_z\ll t_x$,

$$A(\mathbf{p},\mathbf{q},t_x,t_z)\rightarrow C_+(0,\mathbf{p})C_-(0,\mathbf{p}')e^{-E_p(t_x-t_z)}e^{-E_{p'}t_z}$$
$$\times\langle O^-,\mathbf{p}|\rho(0)|O^-,\mathbf{p}'\rangle, \quad (13)$$

with $\mathbf{p}'=\mathbf{p}-\mathbf{q}$. The form factor[12,17] is related to the charge-density matrix element by

$$\langle O^-,\mathbf{p}|\rho(0)|O^-,\mathbf{p}'\rangle=\frac{E_p+E_{p'}}{2\sqrt{E_pE_{p'}}}F(q). \quad (14)$$

For numerical calculations it is convenient to take the ratio[18]

$$\mathscr{R}=\left[\frac{A(O,\mathbf{q},t_x,t_z)A(\mathbf{q},\mathbf{q},t_x,t_z)}{G_0(0,t_x)G_0(\mathbf{q},t_x)}\right]^{1/2}, \quad (15a)$$
$$\xrightarrow[0\ll t_z\ll t_x]{}\frac{E_q+M_0}{2\sqrt{E_qM_0}}F(q). \quad (15b)$$

The three-point function is calculated as the derivative of a two-point function with the charge operator acting as a source.[19] This does not differ in any essential detail from the staggered fermion calculation. The details can be found in Ref. 12.

III. RESULTS

Numerical calculations were done in a model for QCD using only SU(2) color. The lattice was $10\times20\times10\times16$ sites in size with the charge operators carrying momen-

tum in the 2-direction. Eighteen gauge field configurations were used. These were prepared in quenched approximation using the heat-bath Monte Carlo method[20] with the Wilson gauge field action at $\beta=2.3$. The gauge field Monte Carlo was done on a $10^3\times 16$ lattice which was doubled in the 2-direction.

Quark propagators were calculated for one initial space-time point in each gauge field configuration using the conjugate-gradient method.[21] Iterations were carried out on the propagators until the maximum change in the two-point function $G_0(O,t_x)$ at any time point was less than 0.025% in four iterations. The absolute value squared of the residual vectors was less than 10^{-12}–10^{-11}. The calculations used about 20 h on a two-pipe Cyber 205 using half-precision arithmetic.

The same statistical analysis was used here as for the previous study with staggered fermions.[11] For the two-point functions the statistical error at each time step was obtained using the whole sample of eighteen configurations. The error in the meson mass was determined from the error matrix of the least-squares fit of an exponential to the zero-momentum two-point function. Covariances between the different factors in the ratio $\mathscr{R}$ [Eq. (15a)] were included in the statistical error of the form factor. Again all configurations were included in a single sum.

Pseudoscalar- and vector-meson masses for equal-mass quark and antiquark are shown in Fig. 1 as a function of κ^{-1}, the inverse of the hopping parameter. Calculations were done at five values of κ (from 0.134 to 0.158) and the meson masses span about the same range in lattice units as in the calculation with staggered fermions. The solid lines in Fig. 1 are fits used for extrapolation. They will be discussed in the next section.

Figure 2 shows a typical result for the ratio $\mathscr{R}$ of Eq. (15a) versus the time t_x of the meson annihilation operator. The meson creation operator acts at a time (defined to be $t=0$) two steps from the lattice time boundary. The charge density is placed at $t_z=4$. With the time boundary conditions used here, a net charge is present only between

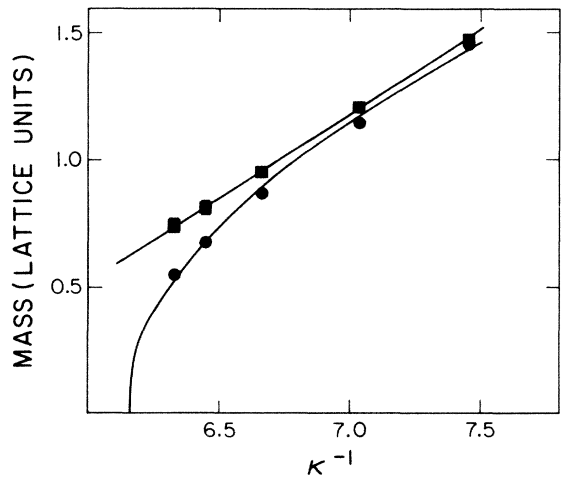

FIG. 1. Pseudoscalar- (●) and vector- (■) meson masses vs the inverse of the hopping parameter. The solid lines are fits described in Sec IV.

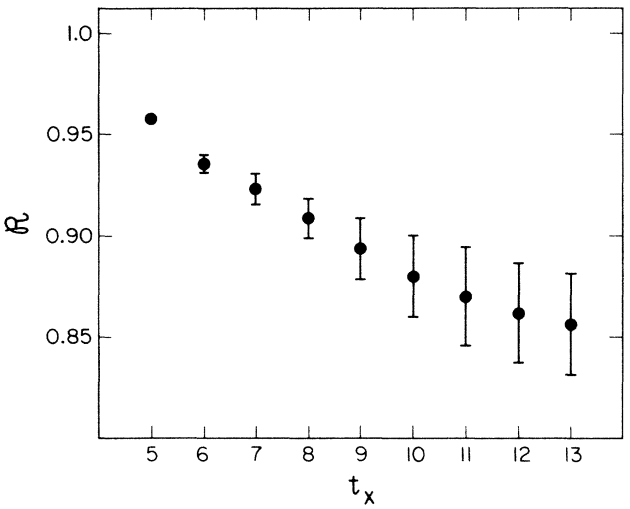

FIG. 2. The combination $\mathscr{R}$ of three- and two-point functions [Eq. (15a)] vs the time coordinate of the meson annihilation operator. The charge-density operator acts between time step 4 and 5.

meson creation ($t=0$) and annihilation ($t=t_x$). When $t_x<t_z$, $\mathscr{R}$ is essentially zero.

In contrast with what was found with staggered fermions the ratio $\mathscr{R}$ is not completely time independent. This should have been anticipated since it was known already from mass calculations in the Wilson scheme that a large time interval is needed before one sees pure single exponential falloff of the two-point function. The time dependence in $\mathscr{R}$ introduces some arbitrariness in the calculation of the form factor. Results presented here were obtained from an average of $\mathscr{R}$ (weighted by statistical errors) for times 8 through 11, i.e., staying away (in time) from both the charge operator and the lattice boundary.[22]

The pseudoscalar-meson electric form factor was calculated for all values of the hopping parameter at one value of momentum transfer, $q=\pi/10$, the minimum nonzero value for 20 lattice sites. For $\kappa=0.150$ the form factor was also calculated at $q=\pi/5$. The form factor for $\kappa=0.150$ is plotted in Fig. 3 as a function of Minkowskian four-momentum transfer squared $Q^2=2M_0[(q^2+M_0^2)^{1/2}-M_0]$.

The form factor values at $q=\pi/10$ are plotted in Fig. 4(a) as a function of κ^{-1}. Larger values of κ^{-1} correspond to larger quark masses. As expected the form factor increases as the quark mass increases. The root-mean-square radius $R_{\rm rms}$ is obtained by first fitting the form-factor values at $q=\pi/10$ with $F(Q^2)=(1+Q^2a^2/\lambda^2)^{-1}$ and then using the relation

$$R_{\rm rms}{}^2=-6\frac{dF(Q^2)}{dQ^2}\bigg|_{Q^2=0}$$

on the monopole fit.[23] The charge radii are shown in Fig. 4(b). In a previous study of the meson form factor it was observed that the parameter λ^2 scales with the vector-meson mass squared, reminiscent of vector-dominance

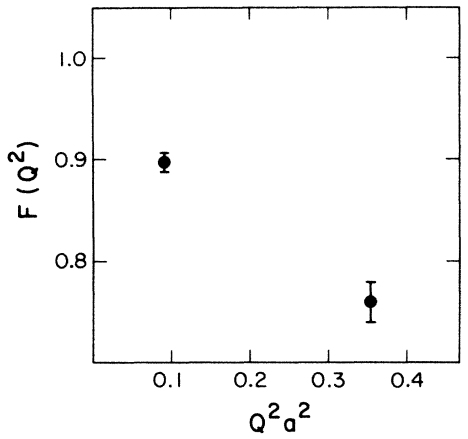

FIG. 3. The pseudoscalar-meson electric form factor vs the Minkowskian four-momentum transfer squared Q^2a^2 for $\kappa=0.150$.

ideas.[24] The same behavior is obtained here. This is shown in Fig. 5 where λ^2 and $\lambda^2/M_1{}^2a^2$ are plotted versus κ^{-1}. Qualitatively the results obtained using Wilson fermions are the same as those using the staggered scheme. In Sec. IV a more quantitative comparison will be made.

In the above calculations a local composite operator was used for the pion, i.e., a quark-antiquark pair was created or annihilated at a point. It is natural to ask whether the choice of a local interpolating field biases the form factor results. A partial answer to the question can be obtained, without having to do any additional fermion matrix inversions, by using an extended composite operator to annihilate the pion. The extended operator

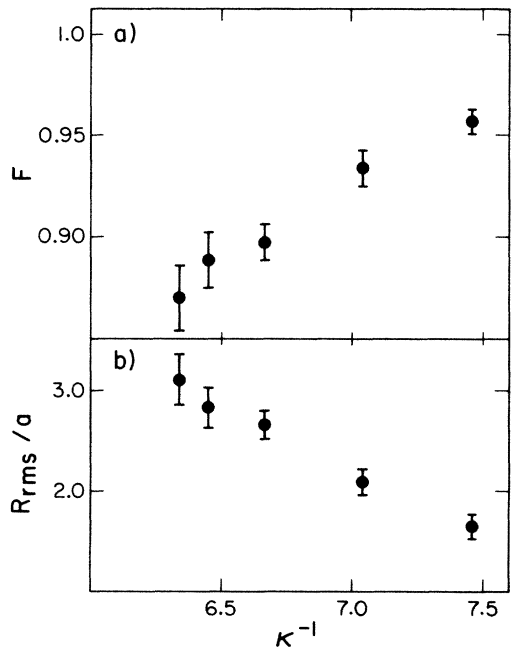

FIG. 4. (a) The pseudoscalar-meson electric form factor at $q=\pi/10$ vs the inverse of the hopping parameter. (b) The meson root-mean-square radius $R_{\rm rms}$ vs the inverse of the hopping parameter.

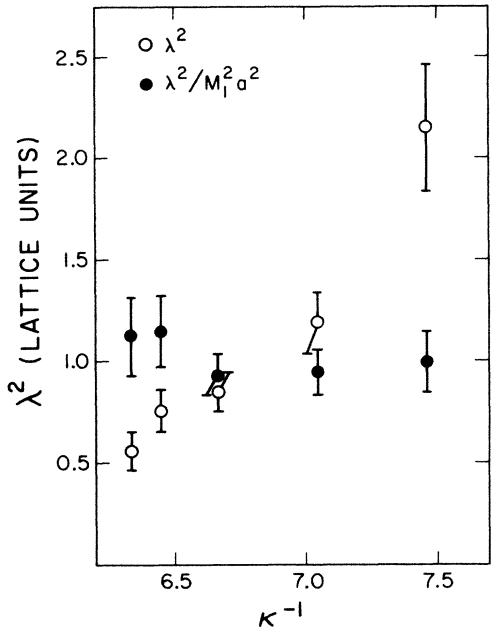

FIG. 5. The λ^2 parameter from a monopole parametrization of the electric form factor vs the quark. The quantity λ^2 is shown both in lattice units (○) and divided by the vector-meson mass squared (●).

$$\tilde{O}_0(x,\nu)=\tfrac{1}{2}\bar{\psi}^u(x)\gamma_5 U_\nu(x)\psi^d(x+a_\nu)$$
$$+\bar{\psi}^u(x+a_\nu)\gamma_5 U_\nu^\dagger(x)\psi^d(x) \quad (16)$$

was used and the form factor was extracted from the three-point function

$$\tilde{A}(\mathbf{p},\mathbf{q},t_x,t_z)=\sum_{\mathbf{x}} e^{-i\mathbf{p}\cdot\mathbf{x}}$$
$$\times\left\langle \tilde{O}_0(x,\nu)\sum_{\mathbf{z}} e^{i\mathbf{q}\cdot\mathbf{z}}\rho(z)O_0^\dagger(0)\right\rangle . \quad (17)$$

The calculation was done at $\kappa=0.150$ with the operator $\tilde{O}_0$ extended in the 1-direction (transverse to $\mathbf{q}$) and the 2-direction (parallel to $\mathbf{q}$). The two-point and three-point functions change substantially in magnitude when the extended operator is used. However, in both cases the form factor agrees, within statistical errors, with the form factor obtained using the local operator.

Finally we consider the situation where quarks of different flavor are not degenerate in mass. A calculation was done fixing one of the quarks at $\kappa=0.134$ and allowing the other κ to increase to 0.158. Form factors were calculated with the charge-density operator acting either on the light or the heavy quark. The result for one unit of momentum transfer ($q=\pi/10$) are shown in Fig. 6. The charge radii extracted from these form factors are plotted in Fig. 7. The physically reasonable result that in a meson with unequal-mass quarks the charge distribution of the heavy quark has a smaller radius than that of the lighter quark is observed. However, in the Wilson case the radius of the heavy-quark distribution does not shrink as dramatically with decreasing light-quark mass as was found in the staggered fermion calculation (see Fig. 8 of

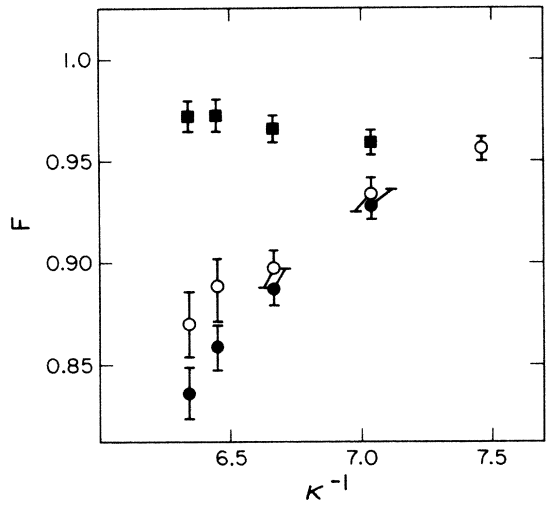

FIG. 6. The electric form factor for the light (●) and heavy (■) quark at $q=\pi/10$ of a pseudoscalar meson with an unequal-mass quark-antiquark pair vs the inverse of the hopping parameter for the light quark. The heavy-quark mass is fixed at $\kappa=0.134$. For comparison the meson form factor in a meson with an equal-mass quark-antiquark pair (○) is also shown.

Ref. 11). This probably indicates that, for the values of κ used here, the ratio of effective quark masses was not as extreme as it was for the staggered fermion calculation.

IV. COMPARISON OF RESULTS WITH WILSON AND STAGGERED FERMIONS

In the continuum limit the Wilson and staggered formulations for lattice fermions should contain the same physics. At finite lattice spacing the chiral properties of the fermions are obviously different so it is clearly interesting to compare the pion structure that emerges with the two schemes. To enable readers to make this comparison in the way they feel is most appropriate a complete enumeration of the results, including those of Ref. 11, is given in Table I.

In lattice units the pseudoscalar mass range covered is about the same in the Wilson and staggered calculations. A superficial examination of Table I clearly shows that the form factors and charge radii are different. However, the different mass splitting between pseudoscalar and vector states observed in the Wilson and staggered schemes shows that different ranges of effective quark mass are being covered in these calculations. Therefore, a direct comparison of the results in lattice units is probably not meaningful.

For a more detailed comparison masses and radii are converted into physical units. The usual procedure for fixing the scale is used here. Masses are extrapolated to the light-quark region, that is, to where a realistic pion and ρ-meson splitting is obtained and the scale (i.e., the lattice spacing a) is set by fitting the ρ-meson mass.

With staggered fermions the meson masses are extrapolated by fitting with the formula

$$\cosh M_J a = A + Bma \tag{18}$$

as was done by Billoire, Lacaze, Marinari, and Morel.[24] The results are shown in Fig. 8. For the pseudoscalar meson (pion)

$$\cosh M_0 a = 1.013(6) + 3.35(4)ma\,, \tag{19}$$

which agrees very well with Ref. 23. The vector-meson mass fit is

$$\cosh M_1 a = 1.50(6) + 3.4(2)ma\,, \tag{20}$$

which is slightly different from that of Billoire, Lacaze, Marinari, and Morel.[24] The end result is a lattice spacing

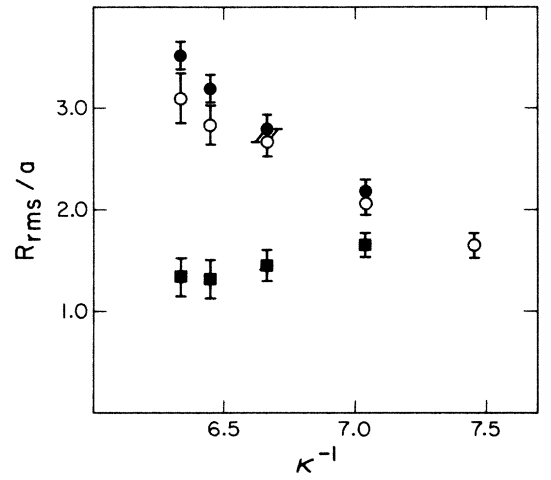

FIG. 7. The root-mean-square radius R_{rms} for the light (●) and heavy (■) quark in a pseudoscalar meson with an unequal-mass quark-antiquark pair vs the inverse of the hopping parameter of the light quark. The heavy-quark mass is fixed at $\kappa=0.134$. For comparison the root-mean-square radius of a meson with an equal-mass quark-antiquark pair (○) is also shown.

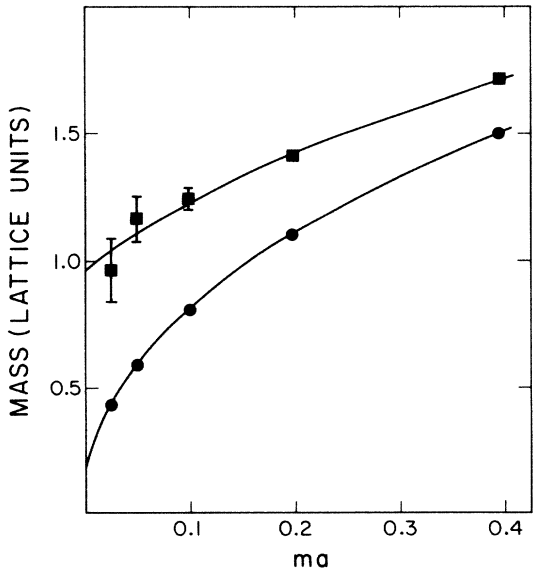

FIG. 8. Pseudoscalar- (●) and vector- (■) meson masses using staggered fermions vs the bare-quark mass. The solid lines are fits described in the text.

TABLE I. (a) Masses and form factors (at $q=\pi/10$) calculated using staggered fermions. (b) Masses and form factors (at $q=\pi/10$) calculated using Wilson fermions.

(a)

ma	M_0a	M_1a	F	$R_{\rm rms}/a$
0.025	0.44±0.02	0.97±0.13	0.930±0.006	2.15±0.11
0.050	0.60±0.01	1.17±0.09	0.948±0.005	1.84±0.10
0.100	0.81±0.01	1.24±0.05	0.954±0.003	1.73±0.06
0.200	1.11±0.01	1.41±0.02	0.965±0.002	1.50±0.04
0 400	1.50±0.01	1.72±0.01	0.978±0.002	1.17±0.06

(b)

κ	M_0a	M_1a	F	$R_{\rm rms}/a$
0.158	0.54±0.02	0.74±0.03	0.87±0.02	3.11±0.24
0.155	0.67±0.02	0.81±0.03	0.89±0.01	2.82±0.20
0.150	0.86±0.02	0.95±0.02	0.90±0.01	2.67±0.13
0.142	1.16±0.02	1.20±0.02	0.934±0.007	2.09±0.12
0.134	1.45±0.02	1.48±0.02	0.957±0.006	1.66±0.12

for the staggered calculation of $a^s=0.24\pm0.02$ fm.

For Wilson the pseudoscalar mass is extrapolated (see Fig. 1) using

$$(M_0a)^2=A_0/\kappa+B_0 \tag{21}$$

with the fitted values $A_0=1.56(4)$, $B_0=-9.6(2)$. This gives $\kappa_c\approx0.162$ as the value where the pion mass vanishes and chiral symmetry, in the Nambu-Goldstone mode, is restored.[2] The vector-meson mass looks completely linear in κ^{-1} and was extrapolated with

$$M_1a=\frac{A_1}{\kappa}+B_1\ . \tag{22}$$

The fitted values are $A_1=0.66(2)$, $B_1=-3.4(1)$. The lattice scale inferred from these values is $a^W=0.157\pm0.005$ fm.

The charge radius $R_{\rm rms}$ vs M_0, now with lattice spacing removed, is shown in Fig. 9. It is encouraging that at smaller meson masses the Wilson and staggered formulations yield compatible results. At larger masses where one gets further away from the Goldstone (or pseudo-Goldstone) behavior of the pseudoscalar meson, there is no reason why the two schemes should give the same meson structures. For completeness the experimental value[25] for the pion charge radius is also shown in Fig. 9 although it is premature to take this comparison very seriously.

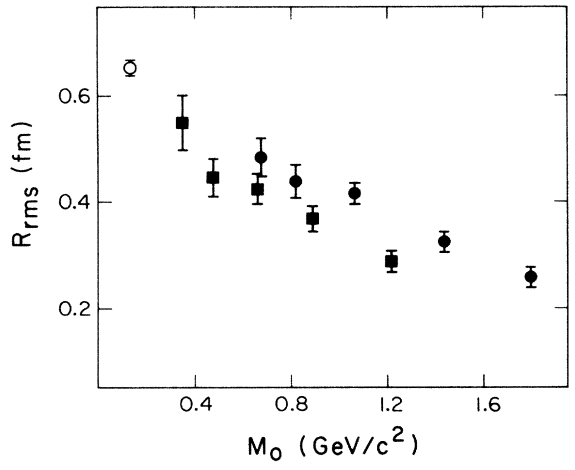

FIG. 9. The root-mean-square radius calculated using Wilson (●) and staggered (■) fermions vs pseudoscalar-meson mass M_0. The experimental value of the pion charge radius is also shown (○).

The reasonable agreement between charge radii (in physical units) calculated with Wilson and staggered fermions came about because of the rather different lattice scales required to fit the meson masses in the two schemes. This is not a very satisfactory situation but also, not unprecedented. In a study of masses with SU(3) color at $\beta=6$ Billoire, Marinari, and Petronzio[8] found a^W to be only slightly larger than a^s. However, at $\beta=5.7$ the staggered fermion results of Gilchrist, Schneider, Schierholz, and Teper[26] give $a^s\approx0.28$ fm while using Wilson fermions Hasenfratz and Montvay[27] found $a^W\approx0.15$ fm. It is possible, therefore, that the discrepancy in scales is the result of being still quite far from the continuum.

V. SUMMARY

In this paper the electric form factor of the pseudoscalar meson (generic pion) was calculated using the Wilson formulation for lattice fermions. The calculations were done in a model for quenched lattice QCD with SU(2) color.

The form factor, calculated for different values of the hopping parameter, clearly shows that the meson size decreases as the quark mass increases. With the parametrization of the form factor at low-momentum transfer $(1+Q^2a^2/\lambda^2)^{-1}$ it was found that the parameters λ^2 scale with the vector-meson mass squared. This is suggestive of the old idea that coupling to vector mesons dominates the low-momentum-transfer behavior of vector-current three-point functions.

The form factor for pseudoscalar mesons with an unequal-mass quark-antiquark pair has also been calculat-

ed. It is found that the distribution of the heavy quark has a smaller radius than that of the light quark, in accord with physical intuition.

The charge radii obtained here using the Wilson scheme are compatible, when converted to physical units, with charge radii previously calculated using staggered fermions. To make the comparison in physical units, lattice scales were fixed by fitting pion and ρ-meson masses. Considerably different lattice sizes were found for the Wilson and staggered calculations possibly indicating that one is still far from seeing continuum behavior.

ACKNOWLEDGMENTS

It is a pleasure to thank B. Dayton for suggesting a sparse matrix multiplication algorithm which led to a highly vectorized conjugate gradient code and A. M. Kobos for his help in getting these calculations done on the University of Calgary SuperComputing Services Cyber 205. I also thank W. Wilcox for helpful discussions. This work was supported in part by the Natural Sciences and Engineering Research Council of Canada.

[1]For a review see M. J. Creutz, *Quarks, Gluons and Lattices* (Cambridge University Press, Cambridge, 1983); C. Rebbi, *Lattice Gauge Theory and Monte-Carlo Simulations* (World Scientific, Singapore, 1983).

[2]L. H. Karsten and J. Smit, Nucl. Phys. **B183**, 103 (1981).

[3]H. B. Nielsen and N. Ninomiya, Nucl. Phys. **B185**, 20 (1981); **B193**, 173 (1981).

[4]K. G. Wilson, in *New Phenomena in Subnuclear Physics,* edited by A. Zichichi (Plenum, New York, 1977), p. 69; Phys. Rev. D **10**, 2445 (1974).

[5]J. Kogut and L. Susskind, Phys. Rev. D **11**, 395 (1975); L. Susskind, *ibid.* **16**, 3031 (1977).

[6]N. Kawamoto and J. Smit, Nucl. Phys. **B192**, 100 (1981).

[7]H. Kluberg-Stern, A. Morel, O. Napoly, and B. Petersson, Nucl. Phys. **B220**, 447 (1983).

[8]A. Billoire, E. Marinari, and R. Petronzio, Nucl. Phys. **B251**, 141 (1985); K. C. Bowler, D. L. Chalmers, A. Kenway, R. D. Kenway, G. S. Pawley, and D. J. Wallace, Phys. Lett. **162B**, 354 (1985).

[9]B. Velikson and D. Weingarten, Nucl. Phys. **B249**, 433 (1985); O. Martin, K. Moriarty, and S. Samuel, *ibid.* **B261**, 79 (1985); K. Barad, M. Ogilvie, and C. Rebbi, Phys. Lett. **143B**, 222 (1984); S. Gottlieb, in *Advances in Lattice Gauge Theory,* edited by D. W. Duke and J. F. Owens (World Scientific, Singapore, 1985), p. 105.

[10]W. Wilcox and R. M. Woloshyn, Phys. Rev. Lett. **45**, 2653 (1985).

[11]R. M. Woloshyn and A. M. Kobos, Phys. Rev. D **33**, 222 (1986).

[12]W. Wilcox and R. M. Woloshyn, Phys. Rev. D **32**, 3282 (1985).

[13]W. Wilcox and K. F. Liu, Phys. Lett. **172B**, 62 (1986).

[14]D. Weingarten, Phys. Lett. **109B**, 57 (1982).

[15]M. Fukugita, T. Kaneko, and A. Ukawa, Nucl. Phys. **B230**, 62 (1984).

[16]C. Bernard, T. Draper, K. Olynyk, and M. Rushton, Nucl. Phys. **B220**, 508 (1983).

[17]C. Itzykson and J. Zuber, *Quantum Field Theory* (McGraw-Hill, New York, 1980), p. 160.

[18]If only one state contributes this removes the times boundary effects and time dependence completely. This ratio can still be used to remove the time dependence even if periodic boundary conditions are used in time. In this case it is necessary to place the operator whose matrix element is being calculated symmetrically about the time origin.

[19]S. Gottlieb, P. B. Mackenzie, H. B. Thacker, and D. Weingarten, Phys. Lett. **134B**, 346 (1984); C. Bernard, in *Gauge Theory on a Lattice: 1984,* edited by C. Zachos, W. Celmaster, E. Kovacs, and D. Sivers (National Technical Information Service, Springfield, VA, 1984), p. 85.

[20]M. Creutz, Phys. Rev. D **21**, 2308 (1980).

[21]F. S. Beckman, in *Mathematical Methods for Digital Computers,* edited by A. Ralston and H. S. Wilf (Wiley, New York, 1960), p. 62.

[22]At larger values of the hopping parameter the behavior of $\mathscr{R}$ near the time boundary ($t_x = 13$) tends to be more erratic. For this reason it was decided arbitrarily to exclude the last two time points from the average for all values of κ.

[23]This procedure is a convenient way of summarizing the low-momentum-transfer behavior of the form factor. It does not imply that the form factor has this exact functional form.

[24]A. Billoire, R. Lacaze, E. Marinari, and A. Morel, Nucl. Phys. **B251**, 581 (1985).

[25]S. R. Amendolia *et al.*, Phys. Lett. **146B**, 116 (1984).

[26]J. P. Gilchrist, H. Schneider, G. Schierholz, and M. Teper, Phys. Lett. **136B**, 86 (1984).

[27]P. Hasenfratz and I. Montvay, Nucl. Phys. **B237**, 237 (1984).